

Inhomogeneity of Spin-Coated and Cast Non-Regioregular Poly(3-hexylthiophene) Films. Structures and Electrical and Photophysical Properties

Masahiro Kobashi* and Hisao Takeuchi

Yokohama Research Center, Mitsubishi Chemical Corporation, 1000 Kamoshida-cho, Aoba-ku, Yokohama 227-8502, Japan

Received April 22, 1998; Revised Manuscript Received August 13, 1998

ABSTRACT: We report structures and electrical and photophysical properties of spin-coated and cast non-regioregular poly(3-hexylthiophene) (P3HT) films. Large differences of the properties are found in these films prepared from different conditions. Results of optical absorption, electron spin resonance, and X-ray diffraction measurements show that the extent of conjugation of P3HT is homogeneous in the spin-coated film, whereas it is inhomogeneous in the cast film. The existence of relatively strong distorted segments with large torsion angles in the thiophene backbone is also suggested, especially in the cast film. Carrier transfer phenomena and unrelaxed exciton diffusion to an emissive singlet polaron exciton are discussed on the basis of proposed structure models of the spin-coated and the cast films.

Introduction

Conjugated polymers have been studied in fundamental interests such as soliton, polaron, and bipolaron in one-dimensional organic electronic systems.¹ Various applied studies have also been reported such as rechargeable battery,² solar battery,³ and field-effect transistor (FET).⁴ Among these applied studies, since the electroluminescence (EL) of poly(para-phenylene-vinylene) (PPV) was discovered,⁵ many studies of EL have been done vigorously. Recently photophysical properties of some conjugated polymers have been studied intensively for revealing the EL mechanism.^{6–8}

In fabrication of thin film devices utilizing conjugated polymers, two kinds of method have been mainly adopted as thin film preparations. One is a precursor polymer route. In this route, a solution of nonconjugated precursor polymer is spun onto appropriate substrates, and then that precursor polymer is converted into a conjugated polymer by thermal or chemical elimination of side groups.^{9,10} Moreover, a sulfonium polyelectrolyte precursor route has been developed in the preparation of PPV.¹¹ This route has been shown to be particularly suitable for manufacturing good quality films. Insoluble and infusible conjugated polymer thin films are thus fabricated by this precursor polymer route. The other is a soluble conjugated polymer route. Soluble conjugated polymers usually have large and long side chains. These side chains affect a conformation of the main chain which dominates a one-dimensional band structure of conjugated polymers. For instance, soluble substituted polythiophenes have colors of EL ranging from blue into near infrared with different substitutions.¹² The soluble conjugated polymer route is of great advantage to the fabrication of thin film devices because of its simple process.

It is generally accepted that structures of soluble conjugated polymers in a solution and in a solid film are complicated. For example, in the solvatochromism and thermochromism of non-regioregular P3HT, it has been reported that a single-chain conformational change

(ordered–disordered transition) occurs.¹³ For a regio-regular poly(3-alkylthiophene) (P3AT), it has been reported that P3AT possessing longer alkyl side chains has a more planar structure, and the aggregation of the long alkyl side chain takes place even in solution.¹⁴ It has also been suggested that the additional long-range ordered structures giving rise to longer conjugated length exist in regio-regular P3AT films.¹⁴ For non-regioregular P3AT films, it has been suggested that the long side chains act as spacers between stacking polymer main chains.^{15,16} Considering these results, the conformation of conjugated main chain would be affected by conditions of the film preparation such as a concentration of solution and a drying process. The conformation of the main chain and the higher-order structures in the solid film must then affect solid-state (bulk) properties such as electrical and photophysical properties. In fact, the electrical conductivity in non-regioregular P3HT film shows different values with about 3 orders of magnitude in different reports.^{17,18} To our knowledge, however, only a few researchers have pointed out that electrical properties depend on film preparation conditions. For example, Assadi et al.¹⁹ have reported that the field-effect mobility of non-regioregular P3HT spin-coated films depends on the structures of thin films influenced by spin-coating conditions. To clear these points is important in a technological aspect to improve performance of the EL and other devices utilizing soluble conjugated polymers.

In this work, we study the extent of conjugation of non-regioregular P3HT and higher-order structures in spin-coated and cast films on the basis of the results of optical absorption, electron spin resonance (ESR), and X-ray diffraction measurements. Electrical and photophysical properties of both films are also reported. The electrical properties are studied by the electrical conductivity and field-effect mobility. The photophysical properties are discussed on the basis of the results of photoluminescence excitation (PLE) spectra.

Experimental Section

Preparation of Samples. P3HT was prepared from 3-hexylthiophene monomer utilizing FeCl₃ as a catalyst. We

* To whom correspondence should be addressed.

followed the procedure of synthesis as described in ref 17. Crude P3HT was vigorously washed by ethanol and filtrated. This procedure was repeated until the filtrate became clear and colorless. The washed P3HT was completely dried up, then dissolved in chloroform and filtrated. Finally, solid P3HT was obtained by solvent evaporation. As shown later, solid films prepared from this purified P3HT showed no absorption peak and no ESR signal, relating to the polaron.²⁰ Therefore, this purified P3HT is the neutral form. P3HT thus synthesized has non-regioregular structures. In this context, P3HT represents "non-regioregular P3HT" without a proviso. The molecular weight distribution of P3HT utilized in this study showed the number-averaged molecular weight (M_n) of about 1.8×10^4 and the weight-averaged molecular weight (M_w) of about 1.5×10^5 by gel permeation chromatography (chloroform as the solvent and polystyrene standard).

In preparation of the spin-coated films, filtered P3HT chloroform solutions at various concentrations were spun onto glass substrates at various spin-coating conditions. For the cast films, filtered 1 mg/mL, 15 mg/mL, and more concentrated P3HT chloroform solutions were cast onto the glass substrates, and then those films were dried up in a capped box. Thicknesses were typically about 2000 Å for the spin-coated film prepared at the condition of 900 rpm spin rate for 30 s with the 15 mg/mL solution, and about 54 000 Å for the cast film prepared from the 15 mg/mL solution. In the following, the spin-coated film prepared from the 1 mg/mL solution at the condition of 900 rpm for 30 s is designated as the 1 mg/mL-900/30 spin-coated film and so on. For the cast film, that prepared from the 1 mg/mL solution is abbreviated to the 1 mg/mL cast film and so on.

Characterization of Samples. The spin-coated and cast films thus fabricated on the glass substrates were used to measure the optical absorption, X-ray diffraction, photoluminescence (PL), and PLE spectrum in air at room temperature. These measurements were carried out utilizing a HITACHI U-4000 spectrophotometer, a RIGAKU RINT-1500, and a HITACHI F-4500 fluorescence spectrophotometer. For the X-ray diffraction measurement, the Cu K α radiation was taken for the incident X-ray beam. The PLE spectrum was measured with the probe wavelength at 710 nm.

For the ESR measurement, each film was peeled off from the glass substrate and then put into an ESR tube. The ESR measurements were carried out by a JEOL JES-FE2XG ESR spectrometer at X-band (9.2 GHz) with 100 kHz field modulation in air at room temperature. The Mn²⁺-MgO solid solution was used as a reference for the g value and the magnetic field calibration. The spin concentration was determined by using a strong coal sample as a standard.

The electrical conductivity was measured by the two-probe method either in air or in vacuo at room temperature. The field-effect mobility in air at room temperature was determined by analyzing a source drain current-voltage characteristic of the field-effect transistor utilizing the P3HT film as a semi-conductive layer and SiO₂ as an insulating layer. The source and drain electrodes were fabricated on top of the SiO₂ insulating layer by a standard photolithographic technique giving the height of 500 Å, the channel length of 50 μ m, and the channel width of 10 mm. The P3HT film was cast onto this substrate as that film covered the source and drain electrodes. These electrical measurements were carried out by a Keithley 617 electrometer/source and a Keithley 237 source measure unit.

Results and Discussion

Optical Absorption. The optical absorption spectra of the P3HT films are shown in Figure 1. Striking differences of the spectra are found in the films prepared from different conditions. For the 15 mg/mL-900/30 spin-coated film, the spectrum shape is similar to that observed in a dilute yellow chloroform solution at room temperature except for the existence of weak shoulder peaks.¹³ The absorption peak maximum (λ_{\max}) and the

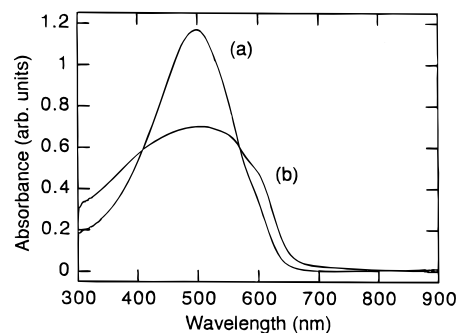


Figure 1. Optical absorption spectra of (a) 15 mg/mL-900/30 spin-coated and (b) 1 mg/mL cast films.

onset of absorption, however, show red shifts as compared with those observed in the dilute chloroform solution at room temperature.¹³

In the solvatochromism and thermochromism of P3HT, it has been reported that the conjugated main chains have only coil-like structure in the dilute yellow chloroform solution at room temperature, and ordered (rodlike) species coexist at low temperature or in solutions containing a poor solvent.¹³ The coexistence of coil-like and rodlike species shows a broad spectrum which clearly differs from that of the dilute solution at room temperature.¹³ Therefore the similarity of the spectrum shape mentioned above suggests that the extent of the conjugation of P3HT in the spin-coated film is homogeneous as in the dilute solution at room temperature. We also conclude that the extent of conjugation of P3HT in the spin-coated film is stronger than that in the dilute chloroform solution, because of the red shifts of the λ_{\max} and the onset of absorption.

The shoulder peaks observed in the spectrum of the spin-coated film are located at about 600 and 550 nm. These shoulder peaks have been considered to arise from the vibronic structure with a 0-0 transition (ca. 600 nm) and a vibronic sideband (ca. 550 nm).¹³ In the solvatochromism of P3HT, it has been reported that these shoulder peaks originate from more ordered species having stronger π -electron orbital overlap between adjacent thiophene rings.¹³ For a regioregular P3HT film, it has also been suggested that the vibronic structure relates to additional long-range ordered structures giving rise to longer conjugation lengths.¹⁴ This vibrational structure in the absorption spectrum has been more clearly observed in poly(*para*-phenylene) (PPP)-type ladder polymers (planarizing PPP) because of a suppression of a rotational degree of freedom.²¹ The appearance of the vibronic structures is thus considered to show the existence of the strong π -conjugation along the main chain. Therefore, we suggest that P3HT in the spin-coated film has some segments with stronger π -electron orbital overlaps between adjacent thiophene rings; namely, more planarized segments exist in the main chain.

For the 1 mg/mL cast film, the relative intensities of shoulder peaks (at ca. 600 and 550 nm) and at shorter wavelength (<500 nm) become stronger than that observed in the spin-coated film. At the same time, considerable broadening of the spectrum shape is observed. These results suggest that the more planarized segments develop and that their fraction also becomes larger in the cast film. This is probably due to slower solvent evaporation during the cast film preparation. We also consider that the extent of conjugation of P3HT

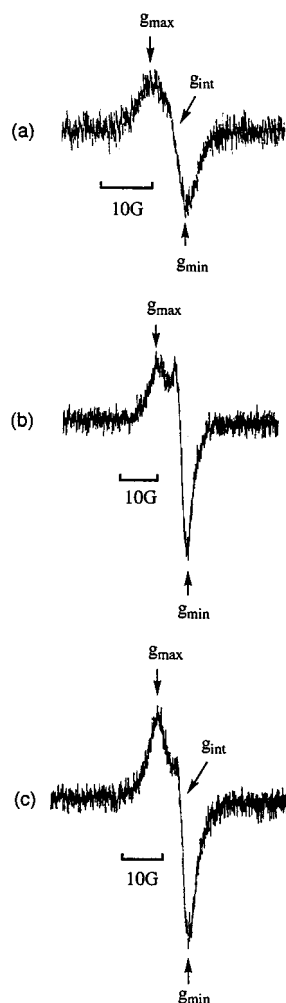


Figure 2. ESR spectra (the first derivative) of (a) 15 mg/mL-900/30 spin-coated, (b) 1 mg/mL cast, and (c) 15 mg/mL cast films. Notations of g_{\max} , g_{int} , and g_{\min} represent the principal values of the g tensor.

Table 1. Principal Values of the g Tensor (g_{\max} , g_{int} , g_{\min}) and Spin Concentration (N_s) of the 15 mg/mL-900/30 Spin-Coated (A), 1 mg/mL Cast (B), and 15 mg/mL Cast (C) Films

films	g_{\max}	g_{int}	g_{\min}	N_s (spins/g)
A	2.0048	2.0022	2.0009	6.0×10^{17}
B	2.0053		2.0006	2.5×10^{17}
C	2.0048	2.0022	2.0008	1.7×10^{17}

in the cast films is inhomogeneous and that its distribution among main chains becomes broader.

ESR. The ESR spectra of the P3HT films are shown in Figure 2. The principal values of the g tensor (g_{\max} , g_{int} , g_{\min}) and the spin concentrations (N_s) are listed in Table 1. The principal values of the g tensor are determined by the maximum, the intercept, and the minimum of the differential curve of the ESR spectra. The observed principal values of the g tensor of all films are in the range of 2.0008–2.0053. The values of N_s of the present films are on the order of about 10^{17} spins/g, which means approximately 1 spin/10000 monomers.

The ESR spectrum of the 15 mg/mL-900/30 spin-coated film shows an asymmetric single line, while that of the 1 mg/mL cast film shows a powder pattern-like signal with anisotropic g values of g_{\parallel} and g_{\perp} . No hyperfine splittings are found in both films. For the 15 mg/mL cast film, the spectrum may consist of two

components: an asymmetric single line such as observed in the 15 mg/mL-900/30 spin-coated film and a powder pattern signal as in the 1 mg/mL cast film.

These observed ESR signals of the P3HT films are quite different from those found in doped/undoped polythiophene,²² poly(3-methylthiophene),²³ and I_2 -doped oligothiophenes.²⁴ For those polymers, it has been reported that the ESR spectra show symmetric single lines with no hyperfine splittings, the shape of which are Lorentzian, Gaussian, or between both types: the observed g values of those ESR spectra are in the range of 2.0020–2.0034. This indicates that the π -radical spins are delocalized on the carbon skeleton in the thiophene backbone. Therefore the anisotropic ESR spectra of the P3HT films suggest that the sulfur atom in the thiophene ring contributes to the behavior of π -radicals, because of the large value of the spin-orbit coupling constant of sulfur. Weak π -electron orbital overlaps are also expected in the thiophene backbone where these π -radicals exist. The observed principal values of g tensor in the P3HT films are, however, somewhat smaller in magnitude than those found for the $R-S^{+}-R$ radical cation (anisotropic g values are typically 2.002, 2.011, 2.004²⁵) where the radical spin is strongly localized on the sulfur atom. The smaller values of g tensor in the P3HT films suggest that the π -radical spins are not completely localized on the sulfur atoms. Therefore we conclude that the π -radical spins in the P3HT films are partially localized on the sulfur $3p\pi$ -atomic orbitals and partially delocalized on the carbon skeleton. We also suggest that the π -radicals in the P3HT films are confined in the strong distorted segments in which the torsion angles between adjacent thiophene rings are relatively large. In other words, this means that the π -radicals exist in the mobility edge in the band structures of the P3HT films.

This confinement effect in the cast film must be stronger than that of the spin-coated film, considering the relatively clear anisotropic ESR signal like the powder pattern found for the cast film. This means that the π -radicals in the cast film exist in deeper states of the mobility edge. The coexistence of the asymmetric single line in the 15 mg/mL cast film, however, suggests that some strongly distorted segments may slightly relax to more conjugated segments with slower solvent evaporation. This result also supports the relatively broad distribution of the extent of conjugation among main chains in the cast film.

X-ray Diffraction. The results of X-ray diffraction measurement of the P3HT films are shown in Figure 3. Note that the broad peaks centered at $\sim 24^\circ$ in all films arise from scattering by the glass substrates.

A very weak peak at 5.25° is observed in the 15 mg/mL-900/30 spin-coated film. This peak corresponds to the first-order reflection from the 16.82 Å parallel spacing of main chains in which the side chains act as spacers.¹⁵ The fraction of this ordered structure in the spin-coated film must be very small. For the cast films, however, this peak is more clearly observed: the corresponding intensity increases as the film is prepared from a more concentrated solution. Moreover, for the 15 mg/mL cast film, the peaks arising from the second- (10.7°) and the third-order (16.2°) reflections from the parallel spacing of main chains¹⁵ are observed. The peak at 23.25° (indicated by the arrow in Figure 3c) which roughly corresponds to the 3.82 Å face-to-face interchain stacking space¹⁵ is also observed. These

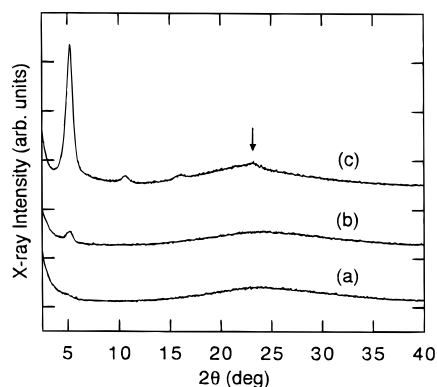


Figure 3. X-ray diffraction pattern of (a) 15 mg/mL-900/30 spin-coated, (b) 1 mg/mL cast, and (c) 15 mg/mL cast films. The arrow in (c) indicates the peak at 23.25° which roughly corresponds to the 3.82 Å face-to-face interchain stacking space (see in the text).

peaks indicate that the two-dimensional sheets consisting of parallel lines with main chains are formed, resulting in the three-dimensional column structures.¹⁵

The intensity of the 5.25° peak increases with the increasing intensity of the shoulder peak at about 600 nm in the optical absorption. This implies that the vibronic structure in the optical absorption relates to the thiophene backbone structure in the parallel lines with main chains. The more planarized thiophene backbone should be formed in the cast film by development of the parallel lines with main chains. It should be noted that the stacking space is found to be 3.82 Å for the 15 mg/mL cast film. This separation should be too large to interact with each main chain as orbital overlapping. Namely, this result indicates that the interchain interaction in the cast film prepared from more concentrated solution is weak.

Model Structures. Summarizing the results of optical absorption, ESR, and X-ray diffraction measurements, we propose model structures of the spin-coated and the cast P3HT films. Model structures of those films are illustrated in Figure 4. For the spin-coated film, the extent of conjugation is relatively homogeneous, and the ordered fraction is very small. These can be deduced from the spectrum shape of the optical absorption and the very weak X-ray diffraction peak. The weak anisotropic ESR signal also indicates that the torsion angles in the distorted segments are relatively small.

For the cast films, the extent of conjugation is more inhomogeneous as suggested by the broad optical absorption spectra. In addition, the distribution of the extent of conjugation among main chains should be broader. On the other hand, the extent of conjugation should become greater on average, because the onset of the optical absorption spectra shows a red shift. The fraction of ordered structures also increases as indicated by the clear X-ray diffraction peaks. However, the strong anisotropic ESR signal implies that the distorted segments having large torsion angles are also created. These large torsion angles of some distorted segments would relax when the cast film is prepared from more concentrated solutions.

Electrical Properties. The electrical conductivities, field-effect mobilities, and carrier concentrations of the 15 mg/mL-900/30 spin-coated and the 15 mg/mL cast films are listed in Table 2. Large differences of the electrical conductivity and the field-effect mobility in air

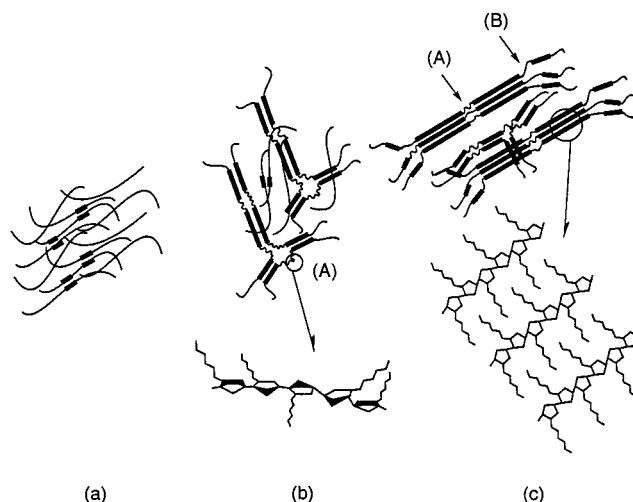


Figure 4. Model structures of the P3HT (a) spin-coated and (b), (c) cast films. (c) shows the cast film prepared under slower solvent evaporation conditions. The bold lines indicate the more planarized and ordered segments in the main chains in (a), (b), and (c). (A) in (b) and (c) represents the distorted segments with large torsion angles between adjacent thiophene rings. (B) in (c) shows a relaxed distorted segment with more conjugation. In (c), the more planarized and ordered segments have the three-dimensional column structures.

Table 2. Electrical Conductivity in Air (σ_{air}) and in Vacuo (σ_{vac}), Field-Effect Mobility (μ), and Carrier Concentration (N) in Air of the 15 mg/mL-900/30 Spin-Coated (A) and 15 mg/mL Cast (B) Films

films	σ_{air} (S/cm)	σ_{vac} (S/cm) ^a	μ (cm ² /Vs)	N (cm ⁻³)
A	1.6×10^{-7}	1.3×10^{-8}	$\sim 10^{-5}$ ^b	$\sim 10^{17}$
B	1.0×10^{-9}	8.2×10^{-10}	1.0×10^{-7}	6.0×10^{16}

^a The condition of evacuation is under 4×10^{-5} Torr. ^b This value is taken from ref 19.

are found between the spin-coated and the cast films. The value of the field-effect mobility of 15 mg/mL-900/30 spin-coated film is taken from ref 19. The carrier concentrations are estimated from the equation $\sigma = Ne\mu$, where σ is the electrical conductivity, N is the carrier concentration, e is the elementary electric charge and μ is the field-effect mobility. The carrier concentrations of both films in air are roughly the same order of magnitude. In air, both the electrical conductivity and the field-effect mobility of the spin-coated film are about 2 orders of magnitude larger than those of the cast film. These results prove that the difference of the conductivity between the spin-coated and the cast films arises from that of the mobility. The lower field-effect mobility of the cast film can be well-interpreted by the proposed model that the cast film has the inhomogeneous extent of conjugation with stronger distorted segments and the weaker interchain interactions. The carrier transfer is thus favorable for the spin-coated film.

Under 4×10^{-5} Torr, the conductivity of the spin-coated film decreases by only 1 order of magnitude. Moreover, the decrement of that of the cast film under the same evacuated condition is very slight. These results show that the effect of oxygen as an acceptor dopant is weak in both films.

Photophysical Properties. The PL spectra of the spin-coated and the cast films showed the same spectrum shape where the peak maximum was located at about 710 nm. The typical PL spectra are shown in Figure 5. It is emphasized that the PL spectrum shape is independent of the excitation energy.

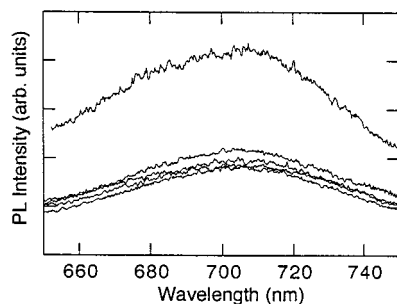


Figure 5. Typical excitation energy dependence of the PL spectrum. Here the spectra of the cast film prepared from 15 mg/mL solution under slower solvent evaporation conditions are shown. Each excitation wavelength is 450, 500, 550, 580, and 620 nm from bottom to top.

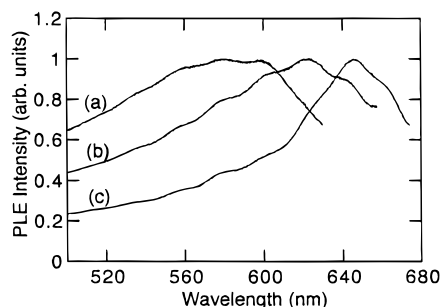


Figure 6. PLE spectra of (a) 15 mg/mL-900/30 spin-coated film, (b) 1 mg/mL cast film, and (c) the cast film prepared from 15 mg/mL solution under slower solvent evaporation conditions.

The PLE spectra of the 15 mg/mL-900/30 spin-coated and the 1 mg/mL cast films are shown in Figure 6. The PLE spectrum of the 15 mg/mL cast film is also shown; this cast film was prepared under slower solvent evaporation conditions. The maxima of PLE intensity for each of the films are normalized to unity for the sake of comparison. In the PLE spectrum of the 15 mg/mL-900/30 spin-coated film, the large 560–600 nm maximum band is observed. Moreover, the relative intensity at the higher excitation energy region (<560 nm) is strong compared with that observed in the cast films.

Rothberg et al.²⁶ have shown that a large fraction of unrelaxed (hot) excitons separates rapidly to form interchain bound polaron pairs and that the remainder diffuses within 1 ps to long conjugation segments by Förster diffusion in PPV. In addition, they have suggested that the singlet polaron excitons that favorably diffuse in one-dimension are quenched at defects such as carbonyl created in PPV by photo-oxidation.²⁶ Shinar⁸ has also pointed out that the interchain bound polaron pairs act as quenching sites for the unrelaxed excitons, and some defects induced by structural disorder enhance the generation of these trapped polarons in PPV and P3AT on the basis of the results of optically detected magnetic resonance measurements. Moreover, for the bound polaron pairs, it has been reported that there is less overlap between the electron and hole wave functions of polarons.⁷ This means that the adjacent chains having the spatial separation favor to create the bound polaron pairs.

Therefore the above-mentioned PLE features of the spin-coated P3HT film indicate that the unrelaxed excitons rather easily relax to the singlet polaron excitons and/or the singlet polaron excitons favorably decay radiatively. As shown in our model structures, the P3HT spin-coated film has the homogeneous extent

of conjugation and the distorted torsion angles in the distorted segments are relatively small. Consequently, the relatively small distorted torsion angles and the homogeneous extent of conjugation in the spin-coated film would hardly result in the trapped polarons as Shinar suggests. In addition, the spin-coated film has no face-to-face interchain stacking as indicated by the X-ray diffraction measurement. This suppresses the formation of the bound polaron pairs. The unrelaxed excitons and the singlet polaron excitons in the spin-coated film thus would hardly be quenched.

For the cast films, the relative intensity at higher excitation energy region (< ca. 620 nm for Figure 6b, < ca. 650 nm for Figure 6c) decreases. This result indicates that the unrelaxed excitons and/or the singlet polaron excitons decay rather nonradiatively. This would arise from the relatively strong distorted segments and the inhomogeneous extent of conjugation in the cast film. Meanwhile, the PLE peak maximum is clearly observed with a red shift. In addition, the PLE peak position becomes close to the absorption edge of the optical absorption. This tendency is well-observed as the film prepared from a more concentrated solution. As described earlier, the cast film has the broad distribution of the extent of conjugation among main chains. Thus the unrelaxed excitons created in *more* conjugated main chains may favor to survive. Such unrelaxed excitons should easily relax to the singlet polaron excitons which are hardly quenched. The 15 mg/mL cast film, in particular, has the 3.82 Å face-to-face interchain stacking space as shown by the X-ray diffraction analysis. This distance is too large to interact with each main chain as orbital overlapping, as mentioned in the section of X-ray diffraction. The interchain bound polaron pairs thus would be easily created, especially in the cast film prepared under slower solvent evaporation conditions. Therefore, in the cast film prepared under that condition, the unrelaxed excitons would mainly be quenched by the interchain bound polaron pairs.

Conclusion

We have reported the structures and electrical and photophysical properties of the spin-coated and the cast P3HT films. Special attention has been paid to the dependence of these properties on the film preparation.

The results of analyses of the optical absorption and ESR spectra have indicated that the extent of conjugation is homogeneous in the spin-coated film, whereas it is inhomogeneous in the cast film. It has also been suggested that both films have the distorted segments with relatively large torsion angles. However, the distorted torsion angles in the cast film are larger than those in the spin-coated film.

The X-ray diffraction results have shown the existence of the parallel lines with main chains in the spin-coated and the cast films, although the fraction of such structures strongly depends on the conditions of film preparations. These parallel lines form the two-dimensional sheets in which the side chains act as spacers. It has been suggested, however, that the face-to-face interchain stacking formed by those two-dimensional sheets only develops under slower solvent evaporation, that is, in the cast film. In addition, the interchain interaction in the cast film prepared from more concentrated solution is weak compared with that in the spin-coated film.

The electrical conductivity and the field-effect mobility have shown quite different values between the spin-coated and the cast films. From these results, we indicated that the carrier transfer is more strongly obstructed in the cast film than in the spin-coated film. This is well-interpreted by our proposed model, in which the cast film has the strongly distorted torsion angles and the weaker interchain interactions.

From the results of the analyses of the PLE spectra, we concluded that the diffusion of unrelaxed exciton and/or the radiative decay of the singlet polaron excitons in main chains are more favorable in the spin-coated film than in the cast film. This behavior arises from the homogeneous extent of conjugation and the relatively small distorted torsion angles in the distorted segments in the spin-coated film. It has also been suggested that the bound polaron pairs are more easily created in the cast films. To study a detailed photo-physical process, the time-resolved photoluminescence measurements are now in progress.

Acknowledgment. We thank K. Sano for fabricating the FET structure by the photolithographical technique and H. Asami for the X-ray diffraction measurement. We also thank O. Shibata and T. Miyata for GPC measurement.

References and Notes

- (1) See, for instance: Heeger, A. J.; Kivelson, S.; Schreiffer, J. R.; Su, W. P. *Rev. Mod. Phys.* **1988**, *60*, 781.
- (2) MacInnes, D.; Druy, M. A.; Nigrey, P. J.; Nairns, D. P.; MacDiarmid, A. G.; Heeger, A. J. *J. Chem. Soc., Chem. Commun.* **1981**, *7*, 317.
- (3) Garnier, F.; Horowitz, G. *Synth. Met.* **1987**, *18*, 693.
- (4) Jarrett, C. P.; Friend, R. H.; Brown, A. R.; de Leeuw, D. M. *J. Appl. Phys.* **1995**, *77*, 6289.
- (5) Burroughes, J. H.; Bradley, D. D. C.; Brown, A. R.; Marks, R. N.; Mackay, K.; Friend, R. H.; Burn, P. L.; Holmes, A. B. *Nature* **1990**, *347*, 539.
- (6) Yan, M.; Rothberg, L. J.; Papadimitrakopoulos, F.; Galvin, M. E.; Miller, T. M. *Phys. Rev. Lett.* **1994**, *72*, 1104.
- (7) Hsu, J. W. P.; Yan, M.; Jedju, T. M.; Rothberg, L. J.; Hsieh, B. R. *Phys. Rev. B* **1994**, *49*, 712.
- (8) Shinar, J. *Synth. Met.* **1996**, *78*, 277.
- (9) Edwards, J. H.; Feast, W. J. *Polymer* **1980**, *21*, 595.
- (10) Ballard, D. G. H.; Courtis, A.; Shirley, I. M.; Taylor, S. C. *Macromolecules* **1988**, *21*, 294.
- (11) See, for instance: Murase, I.; Ohnishi, T.; Noguchi, T.; Hirooka, M. *Synth. Met.* **1987**, *17*, 639.
- (12) Berggren, M.; Inganäs, O.; Gustafsson, G.; Rasmussen, J.; Andersson, M. R.; Hjertberg, T.; Wennerström, O. *Nature* **1994**, *372*, 444.
- (13) Rughooputh, S. D. D. V.; Hotta, S.; Heeger, A. J.; Wudl, F. *J. Polym. Sci., Polym. Phys. Ed.* **1987**, *25*, 1071.
- (14) McCullough, R. D.; Lowe, R. D.; Jayaraman, M.; Anderson, D. L. *J. Org. Chem.* **1993**, *58*, 904.
- (15) Winokur, M. J.; Wamsley, P.; Moulton, J.; Smith, P.; Heeger, A. J. *Macromolecules* **1991**, *24*, 3812.
- (16) Hsu, W. P.; Levon, K.; Ho, K. S.; Myerson, A. S.; Kwei, T. K. *Macromolecules* **1993**, *26*, 1318.
- (17) Sugimoto, R.; Takeda, S.; Yoshino, K. *Chem. Express* **1986**, *1*, 639.
- (18) Morita, S.; Zakhidov, A. A.; Kawai, T.; Araki, H.; Yoshino, K. *Jpn. J. Appl. Phys.* **1992**, *31*, L890.
- (19) Assadi, A.; Svensson, C.; Willander, M.; Inganäs, O. *Appl. Phys. Lett.* **1988**, *53*, 195.
- (20) See, for instance: Hotta, S.; Rughooputh, S. D. D. V.; Heeger, A. J.; Wudl, F. *Macromolecules* **1987**, *20*, 212.
- (21) Graupner, W.; Grem, G.; Meghdadi, F.; Paar, C.; Leising, G.; Scherf, U.; Stelzer, F. *Mol. Cryst. Liq. Cryst.* **1994**, *256*, 549.
- (22) Kaneto, K.; Hayashi, S.; Ura, S.; Yoshino, K. *J. Phys. Soc. Jpn.* **1985**, *54*, 1146.
- (23) Tanaka, K.; Sichiri, T.; Yoshizawa, K.; Yamabe, T.; Hotta, S.; Shimotsuma, W.; Yamauchi, J.; Deguchi, Y. *Solid State Commun.* **1984**, *51*, 565.
- (24) Tanaka, K.; Matsuura, Y.; Oshima, Y.; Yamabe, T. *Synth. Met.* **1994**, *66*, 295.
- (25) Kominami, S. *J. Phys. Chem.* **1972**, *76*, 1729.
- (26) Rothberg, L. J.; Yan, M.; Papadimitrakopoulos, F.; Galvin, M. E.; Kwock, E. W.; Miller, T. M. *Synth. Met.* **1996**, *80*, 41.

MA980632U